

# **Modelling of Helicopter Noise in Arbitrary Maneuver Flight using Aeroacoustic Database**

Anne Le Duc<sup>1</sup>, Pierre Spiegel<sup>1</sup>, Frédéric Guntzer<sup>1</sup>,  
Markus Lummer<sup>1</sup>, Joachim Götz<sup>2</sup>

<sup>1</sup> DLR in der Helmholtz Gemeinschaft,  
Institute of Aerodynamics and Flow Technology, Technical Acoustics Division,  
Lilienthalplatz 7, 38108 Braunschweig, Germany

<sup>2</sup> DLR in der Helmholtz Gemeinschaft,  
Institute of Flight Systems, Helicopter Division,  
Lilienthalplatz 7, 38108 Braunschweig, Germany

Corresponding author: Frederic.Guntzer@dlr.de  
Phone number: +49 531 295 3306  
Fax number: +49 531 295 2320

## **ABSTRACT**

This paper presents a computational tool to predict the ground noise footprint of a complete helicopter in an arbitrary flight (including maneuvers). It relies on a hybrid approach: generation of an arbitrary trajectory, checks of flyability and comfort, and propagation of noise down to the ground are performed numerically. On the other hand, noise emission characteristics are provided by a database generated from aeroacoustic flight tests (PAVE 2004). The underlying idea is that the instantaneous noise emission of the whole helicopter can be characterized by the instantaneous value of few aerodynamic parameters. The paper presents a step-by-step validation of the approach and shows ground noise footprint in good agreement with experimental data.

**Keywords** : Aeroacoustics, flight mechanics, noise abatement flight procedures, helicopter

## NOTATION

A complete list of all variables relating to helicopter aerodynamics and acoustics with exhaustive definition can be found on "www.dlr.de/as/Friendcopter-dictionary". We list here the principal variables needed for this article. Fig 1 and 2 show respectively the helicopter coordinate system and a terrain coordinate system.

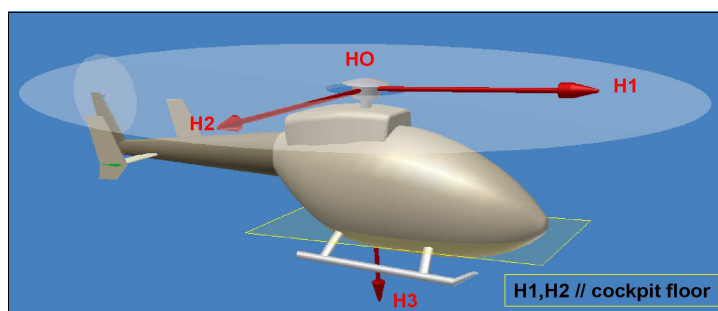


Fig. 1: Axes (H1,H2,H3) and reference point (rotor head center of the main rotor, HO) of the helicopter coordinate system H.

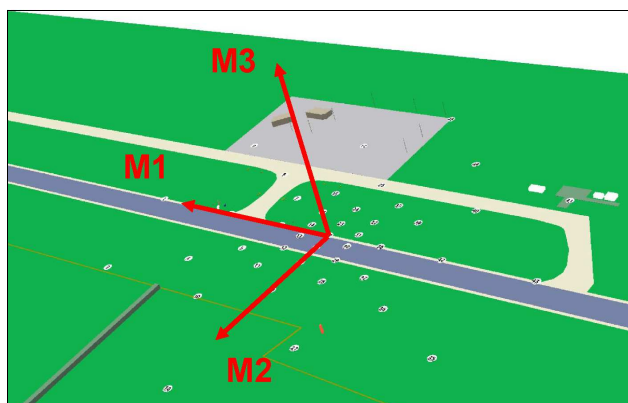


Fig. 2: Axes (M1,M2,M3) and reference point (MO) of the microphone coordinate system (M, one of the terrain coordinate systems).

Name	Symbol	Signification
beta	$\beta$	Side slip angle
alpha	$\alpha$	Fuselage angle of attack
Vz		Climb rate
PmAlpha	$\alpha_{Pm}$	Tip path plane angle of attack (for main rotor)
RmCT	$CT_{Rm}$	Main rotor thrust coefficient
RmMu	$\mu_{Rm}$	Main rotor advance ratio
PtAlpha	$\alpha_{Pt}$	Tip path plane angle of attack (for tail rotor)

RtCT	$CT_{Rt}$	Tail rotor thrust coefficient
RtMu	$\mu_{Rt}$	Tail rotor advance ratio
s		Parametrization of the trajectory
phi	$\phi$	Roll (or bank) angle
theta	$\theta$	Pitch angle
psi	$\psi$	Heading angle
dphidt	$d\phi/dt$	Rate of roll
dthetadt	$d\theta/dt$	Rate of pitch
dpsidt	$d\psi/dt$	Rate of yaw
P		Rotational velocity along H1
Q		Rotational velocity along H2
R		Rotational velocity along H3
EmRec		Vector from emission point to reception point
theta3	$\theta_3$	First directivity angle (angle between H3 and EmRec)
phi3	$\phi_r$	Second directivity angle (angle between H1 and the projection unto H1H2 of EmRec)

## INTRODUCTION

For helicopter manufacturers and users, the helicopter noise perceived on ground is a major concern. This noise problem can be alleviated by designing new helicopters (through purposeful blade design or active control), or by designing flight procedures which minimize the noise perceived on ground. The helicopter group of the technical acoustic division of DLR has been involved in the second strategy for several years. Flight test campaigns and projects have been designed to progress on this topic [12,13,17,18].

This paper presents a method able to design arbitrary flights, evaluate their flyability, and compute their ground noise footprint. The method will be later used to design noise abatement flight procedures. The following physical phenomena should be taken into account:

- All noise components of the helicopter should be included in the noise evaluation method: main rotor, tail rotor, engines. Indeed, although the main rotor noise is dominant for certain flight conditions (typically the noise certification 6 deg. descent), the fenestron noise, for instance, can dominate the noise for steep descents [12].
- The tool should be able to compute maneuver noise. In their numerical study of main rotor noise, Perez et al. [6] report for a deceleration of 0.1 g a noise reduction up to 20 dB in frequencies within 6 to 40 blade passage frequency. The difference in noise level can be explained by a change in the angle of attack of the main rotor, one of the parameters known to characterize BVI

[15]. Avoidance of BVI using small decelerations offers potential for the design of noise abatement flight procedures.

- The effect of wind should be taken into account. Given a glide slope relative to ground, the presence or absence of wind changes the glide slope with respect to air, leading to a different trim and a different angle of attack of the main rotor tip path plane. Thus the noise emission in the presence of wind can differ from the case without wind [10]. Additionally, wind affects noise propagation. Within this paper, we take into account the effect of wind on emission (mainly via its effect on the angle of attack of the main rotor tip path plane and the advance velocity) but neglect its effect on propagation.
- The whole flight envelope in steady and unsteady flight conditions should be covered.
- Avoidance of vortex ring state (VRS) and of forbidden regions in the H-V diagram (safety requirement in case of engine failure) should be ensured. Criterion of comfortable flight should be included.

Based on this list of features, a purely numerical tool is excluded because of its present inability to take into account all noise sources for flights including maneuvers. On the other hand, a purely experimental approach is also excluded because of the costs involved. The helicopter group of the technical acoustic division of DLR has thus been developing a hybrid approach for several years. It combines aeroacoustic in-field flight tests (to characterize the acoustic emission of given flight conditions) and simulation (to assemble them in order to obtain the noise of new procedures).

Performing a noise footprint minimization starts with prescribing any flight procedure by few control points (where the helicopter position and velocity are specified), and then assessing its noise perceived on ground. Subsequently, an optimizer can be used to adjust the control points so that the noise footprint is minimized. This paper focusses on the development of trajectories parametrized by control points and on the computation of their ground noise footprint. We use the acoustic flight-test campaign performed in 2004 in DLR PAVE project and described in [12]. The method is tested on the EC135-FHS but also applies to helicopters of all types. The paper is organized as follows: in the next section, we explain the principle of the computational tool for computation of the ground noise footprint of an arbitrary flight. The required aeroacoustic database, linking flight conditions to noise emission (noise intensity as function of spatial direction and frequency), is covered in the following section. The last section devotes to a detailed description of the computational chain and its step-by-step validation.

## **OVERVIEW OF THE COMPUTATIONAL CHAIN**

Our goal is to compute the noise created on ground by an arbitrary trajectory. We explain in section "Computing the noise of an arbitrary trajectory" how an arbitrary trajectory can be defined in a general manner using control points (quadruplets of Cartesian coordinates and velocities governing the complete flight path). For the moment, we focus on the computation of noise.

### **PRINCIPLE**

Ground noise results from an emission and a propagation down to ground. For the propagation, we take numerically into account spherical spreading, atmospheric absorption, ground effects and Doppler effect. For the noise emission, we rely on experimental data.

The key idea is to characterize the noise emission by the *instantaneous* value of some aerodynamic parameters, so-called noise emission parameters. We consider that if those parameters are equal in two flights (even if other parameters, for instance glide slope, differ) then the noise emission in the helicopter coordinate system H is the same. Consequently the data collected from one flight can be used for the other. The idea is thus to collect noise emission directivities (i.e. noise intensity as function of emission direction and emission frequency) together with noise emission parameters for a large variety of flight conditions. All noise emission patterns are stored in a database and referenced by their noise emission parameters. Furthermore we assume that if a combination of values of the noise emission parameters has not been measured, then its noise emission can be interpolated from the noise emission of neighboring conditions. The success of the approach depends on the choice of the noise emission parameters, on the density of measured noise emissions and on the interpolation procedure. We now focus on the choice of the noise emission parameters.

We want to characterize the noise of the complete helicopter in maneuver in the presence of wind. As the external noise is an aerodynamic phenomenon, the noise emission parameters should be aerodynamic. Additionally, we want to investigate flights that will be truly flown in operation. Thus those flights should satisfy flyability and comfort condition. The second condition is equivalent with stating that the maneuvers should remain mild: high values of linear and especially angular accelerations are excluded. We call this condition "quasi-steadiness". Under this condition, we can assume that noise emission can be characterized by the instantaneous values of aerodynamic parameters already found relevant for noise emission in steady flight conditions. Wind tunnel experiments and

theoretical studies on BVI (Blade Vortex Interaction) [15] and on HSI (High Speed Impulsive) noise [8,11] have shown that the noise emission of the main rotor depends on its advance ratio  $\mu_{Rm}$ , its thrust coefficient  $CT_{Rm}$  and its tip path plane angle of attack  $\alpha_{pm}$ . Addition of the helicopter side-slip angle  $\beta$  allows to parametrize the noise emitted by the complete helicopter. For justification, see [4,12]. Because of costs, the flight test performed in PAVE 2004 were restricted to values of  $\beta$  usually close to zero. In this paper we thus restrict to simulations with  $\beta$  close to zero. The set of noise emission parameters thus finally read:  $\alpha_{pm}$ ,  $CT_{Rm}$ ,  $\mu_{Rm}$ .

## FLOWCHART

We now explain briefly the different steps of the computation of the ground noise footprint. Fig. 3 offers a schematic representation of the computational chain. Details of each module are provided in the section “Computing the noise of an arbitrary flight”.

- In order to compute the ground noise, we first define the position of the ground points (Cartesian coordinates) where the noise will be computed. We alternatively refer to those points as microphone carpet.
- We prescribe atmospheric conditions (including wind).
- We define a trajectory. Therefor we define control points as quadruplets of Cartesian coordinates and velocity magnitude (with respect to ground) of the helicopter. The continuous trajectory is built using those control points. We then perform comfort and flyability checks on this trajectory to ensure that it can be later flown. This requires a flight mechanics program (in our case, HOST [2], provided by Eurocopter). The flyability and comfort checks take the wind into account.
- For emission instants taken every 1 sec. on the trajectory, we compute the value of the noise emission parameters with the flight mechanics program, taking the wind into account.
- Then a loop (in time) is run on the set of emission instants. For each emission instant, we compute the directivity angles for each point of the microphone carpet. The noise emission corresponding to the noise emission parameters is retrieved: we search in the database the closest sets of noise emission parameters. Let us assume we have 4 closest neighbors. For each of those neighbors, the noise emission in the direction of the carpet microphone is first computed. The final spectrum is the weighted sum of those four values.
- This noise is propagated down to the ground, taking into account spherical spreading, atmospheric propagation, ground effect and Doppler effect. For each carpet microphone, the noise spectrum is thus known as function of the reception time. Further postprocessing (LdBA, SEL levels...) are then performed.

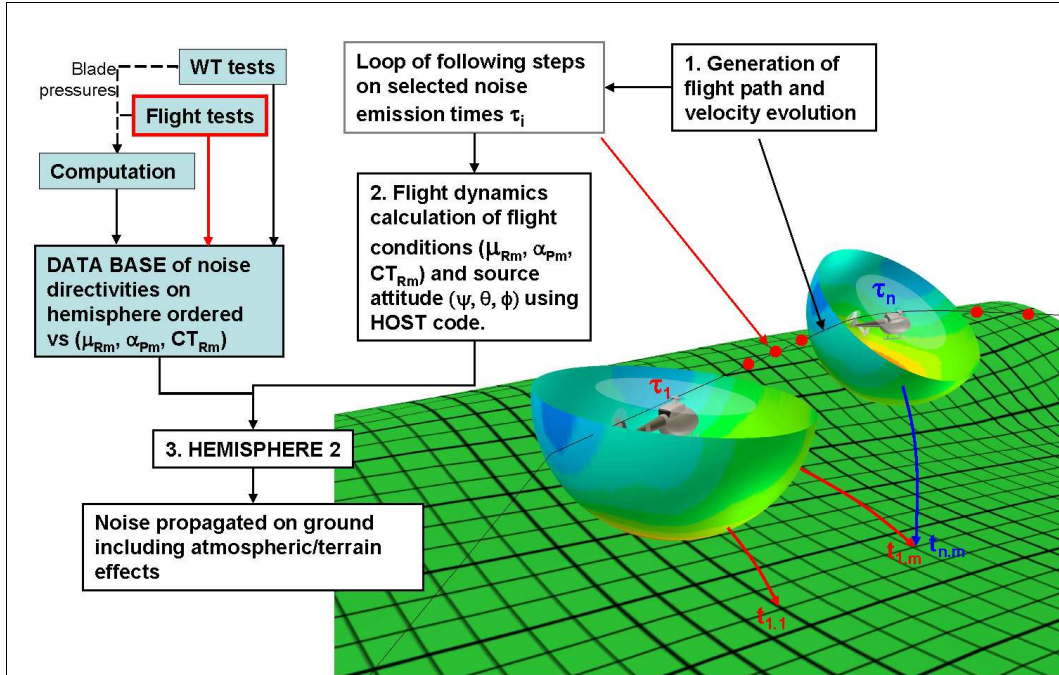


Fig. 3: Schematic representation of the computational chain.

## AEROACOUSTIC DATABASE

The previously described computational chain relies on the existence of a database providing the noise emission characteristics as function of flight conditions. For this paper, the database has been obtained through flight tests. For an exhaustive description of these PAVE 2004 flight tests, refer to Spiegel et al. [12].

The aeroacoustic database associates a noise emission directivity (noise level as function of emission direction and emission frequency) to a set of noise emission parameters. First we explain how the noise emitted by the helicopter can be deduced from ground acoustic measurements using propagation models including spherical spreading, atmospheric absorption, ground effect and Doppler effect. Then we explain how the noise emission parameters are obtained. We conclude with the scope of noise emission parameters available in the database.

## ACOUSTIC DATA

We wish to obtain the sole *noise emission* of a given flight condition. As we use acoustic data collected with microphones placed on ground, we need to remove from the data all effects of propagation (spherical spreading, atmospheric attenuation, ground effect, Doppler effect). We explain here this backpropagation procedure.

The microphone layout used during the PAVE tests counts 43 microphones placed on grass or on concrete, all set head down. The layout allows to collect the instantaneous noise emission with a good directivity coverage when the helicopter is approximately above the center of the microphone carpet.

In order to remove effects of propagation, the noise (fine bands) collected at different reception times is backpropagated onto a fictitious sphere centered at the rotor hub with radius 1m. The direction on this sphere is described with the two angles  $\theta_3$  and  $\phi_3$ , defined in the helicopter coordinate system H. See section “Notation”. In the backpropagation procedure, we assume that the atmosphere is quiet and homogeneous (humidity 80%) and that the ground is flat. Spherical spreading and atmospheric absorption (using Sutherland law [1]) are taken into account. In order to avoid spurious amplification of background noise, ground sound pressure levels whose intensity is smaller than the background noise (assessed to be 30 dB) are set to zero. For the frequencies, the Doppler effect is removed.

Ground effect depends on the medium surrounding the microphones: according to whether they are placed on grass or concrete, microphones can record differences in noise level (after removal of atmospheric propagation and spherical propagation) of about 10 dB for grazing incidence [12]. This is attributed to the attenuating effect of grass and to complex interference patterns due to the experimental setup. For incidences close to normal, no such problem is observed. We took the ground effect into account by specifying whether a ground microphone is set on grass or on concrete. For microphones placed on grass, ground attenuation factors are provided by the experimental calibration described in Pott-Pollenske et al. [7] for the same microphone setup. There, attenuation factors have been measured for incidence angles (with respect to ground) greater than 15 deg. If the incidence angle is smaller, the attenuation factor for the same frequency and the incidence angle equal to 15 deg is used. For microphones set on concrete, the Ingard-Rudnick model [9] is used together with a Delany-Bazley absorber model [3] for the ground. The specific flow resistivity is set to  $200000 \text{ kN.s.m}^{-4}$  for concrete.

## NOISE EMISSION PARAMETERS

Although numerous variables were recorded on board during the flight test campaign (velocity of local air using a probe placed at the tip of a nose boom, helicopter attitude angles  $\psi$ ,  $\theta$ ,  $\phi$ , linear acceleration and rotational velocities with an inertial platform for instance), not all noise emission parameters could be directly recorded on board (for instance  $\alpha_{pm}$  is missing). We obtained them with a flight mechanics program (HOST, [2]).

The conventional way to use a flight mechanics program consists in inputting the four pilot commands (or equivalently the swashplate collective pitch, the two cyclic pitches, and the tail rotor pitch) as function of time and getting as output all flight variables as function of time. During the flight campaign [12], those variables could unfortunately not be recorded continuously because of a partial failure of instrumentation. Thus the flight mechanics program could not be run in this usual manner. Fortunately HOST offers a so-called inverse mode. It consists in prescribing as function of time some target values of four objective variables. The program finds iteratively appropriate values of the 4 pilot commands so that the computed values converge to the target values. The success of the procedure depends sensitively on the choice of objective variables. See [4] for further explanations. Best results are obtained for a simple link between pilot commands and objective variables. The two cyclic pitches of the main rotor and the tail rotor pitch strongly influence the three rotational velocities P, Q, R of the helicopter while the main rotor collective pitch governs the vertical linear acceleration (and accordingly the vertical linear velocity Vz). Thus P, Q, R and Vz are chosen as objective variables. The inverse simulation allows to obtain the complete usual output of HOST, including all noise emission parameters: the main rotor tip path plane  $\alpha_{pm}$ , the main rotor advance ratio  $\mu_{Rm}$  and the main rotor thrust coefficient  $CT_{Rm}$ . Note that many parameters influence the values obtained. We discuss the influence of wind and of helicopter mass.

## INFLUENCE AND EVALUATION OF WIND

HOST requires the input of wind or of the velocity of undisturbed air with respect to helicopter. This last variable is in principle measured with a 3D-velocity probe placed on a nose boom. Unfortunately, the nose boom does not place the velocity probe completely outside the helicopter induced velocity field [12]. Computations are thus performed with the DLR panel code UPM [16] to evaluate the rotor induced velocity; we assume that the velocity induced by the fuselage is negligible at nose boom. The computation of the rotor induced velocity is performed for 8 flight conditions representative for the whole campaign. We use an interpolation procedure to obtain the correction for all measured flights. Details are provided in [4]. The method typically corrects the angle of attack within 1 deg.

## EFFECT OF VARIABLE MASS

The helicopter mass varies during the campaign because of fuel consumption. Tests conducted with the flight mechanics program on a maneuver flight have shown that, when the mass varies by 40 %,  $\alpha_{pm}$  varies by 1deg , and  $CT_{Rm}$  varies by 50 %. The actual mass is set constant for a given flight but varies from flight to flight based on the level of the fuel tanks.

The change of mass also changes the position of the center of gravity which is thus not known. In the simulation, setting this position to a wrong value can lead to offsets in the attitude angles  $\phi$  and  $\theta$  of about 3 degrees. The angle of attack of the tip path plane remains correct, but because theta and phi are wrong, the attitude of the tip path plane with respect to the fuselage is wrong. As the noise hemispheres are stored in the helicopter coordinate system H, there is an offset on the directions. In HOST, we adjust the position of the gravity center along H1 (respectively H2) so that the computed and measured mean values of  $\theta$  (respectively  $\phi$ ) match.

## EXTENT OF AEROACOUSTIC DATABASE

Repeating the procedures explained above for all flights flown during the 2004 PAVE campaign, we dispose of an aeroacoustic database associating noise emission to set of noise emission parameters. For the EC135 FHS 243 flyovers were measured. The present database has been generated using all flyovers except 3 dimensional flight paths and turns: 205 flyovers were used and several instants can be used to build directivity spheres during a flyover. The database thus contains approximately 3400 sets of noise emission parameters, with the corresponding noise emission spectra in all measured directions. Fig 4 shows a three dimensional view ( $\mu_{Rm}$  as function of  $\alpha_{pm}$  and  $CT_{Rm}$ ) of all measured sets of noise emission parameters. Fig. 5 shows two dimensional projections.  $\alpha_{pm}$  varies between -24 deg and +36 deg,  $\mu_{Rm}$  between 0.07 and 0.31, and  $CT_{Rm}$  between 0.0033 and 0.008. We thus have an extensive aeroacoustic database covering the whole flyable steady state domain and a large variety of maneuver conditions. It is adequate for the noise evaluation of arbitrary flyable and comfortable flights.

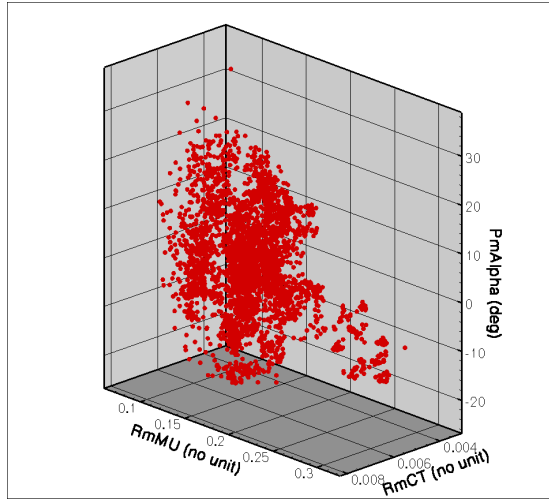


Fig. 4: Representation of all sets of noise emission parameters measured during the PAVE 2004 campaign for the EC135-FHS. Three dimensional view.

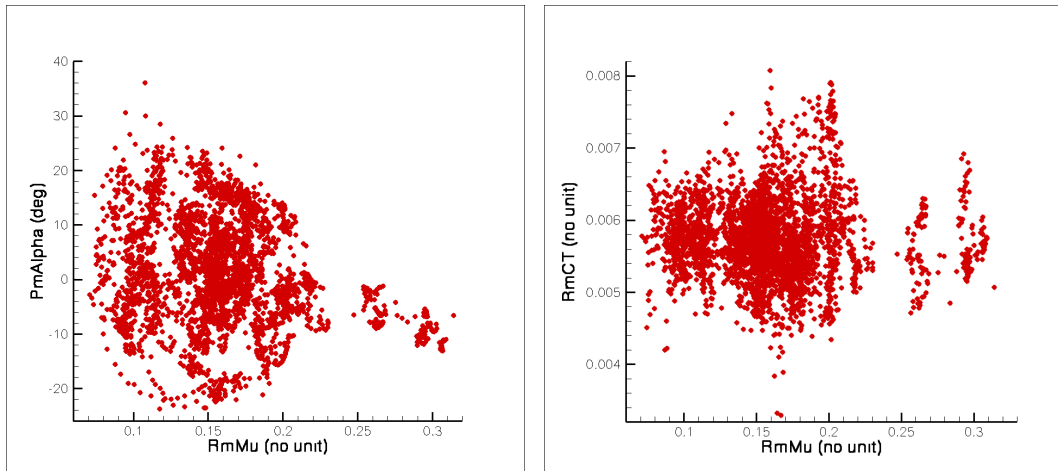


Fig. 5: Representation of all sets of noise emission parameters measured during the PAVE 2004 campaign for the EC135-FHS. Two dimensional views in the plane  $(\mu_{Rm}, \alpha_{Pm})$  (left) and  $(\mu_{Rm}, CT_{Rm})$  (right) are shown.

## COMPUTING THE NOISE OF AN ARBITRARY FLIGHT

We now focus on the computation of the noise generated by an arbitrary flight. We detail the steps mentioned in the "Overview of the computational chain", section "Flowchart" and validate each of them separately. We explain how we generate a flight satisfying flyability and comfort criteria. We then turn to the computation of the noise emission parameters along the trajectory. The next section explains the proper selection of noise emission spheres and interpolation procedures. We finally compare noise footprints measured experimentally with noise footprints computed with the aeroacoustic database.

### GENERATION OF A TRAJECTORY

We recall that our final goal is to optimize trajectories to minimize their noise. In order to keep the optimization procedure feasible, we must limit the number of degrees of freedom of the design space. Thus, instead of considering the infinite number of points forming a trajectory, we prescribe each trajectory by a set of control points. The continuous trajectory is obtained by interpolation between those control points. We present and compare two strategies therefor: one relies on quintic splines, the other on Bézier cubic curves.

Boundary conditions on a complete flight are usually the Cartesian position and velocity with respect to ground of the helicopter at start and end points. Thus we choose those variables as control parameters. Besides, the total duration of a flight is usually not strictly known: we parametrize the trajectory by a parameter „ $s$ “ (a curvilinear abscissa). The trajectory is fully described by  $x(s)$ ,  $y(s)$ ,  $z(s)$ ,  $V(s)$ , where  $x$  (respectively  $y$ ,  $z$ ) is the Cartesian position of the rotor head center along M1 (respectively M2, M3) and  $V$  is the magnitude of the velocity with respect to ground of the rotor head center. At each of the  $N$  control points  $s_i, i \in (1, N)$ ,  $x(s_i), y(s_i), z(s_i), V(s_i)$  should match the prescribed control values  $x_i, y_i, z_i, V_i$ . The task is now to obtain  $x(s)$ ,  $y(s)$ ,  $z(s)$  as functions of time. In order to have a trajectory compatible with helicopter flight dynamics and minimize potential instabilities of HOST, we decided to limit our investigations to procedures with differentiable acceleration. This requires that  $x$ ,  $y$  and  $z$  are at least three times differentiable functions of  $s$  and that  $V$  is a twice differentiable function of  $s$ . Time results from the specification of  $x(s)$ ,  $y(s)$ ,  $z(s)$  and  $V(s)$ .

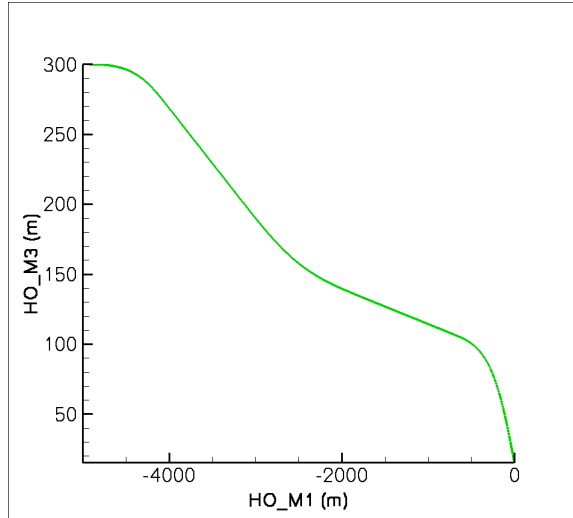


Fig. 6: Example of a trajectory generated from control points and quintic splines: altitude of helicopter versus horizontal distance to landing point. Seven control points have been used. The acceleration is set to zero between the second and third control points, and between the fourth and fifth control points.

Using quintic splines for  $x$ ,  $y$ ,  $z$  and  $V$  clearly allows to satisfy a priori that the acceleration is differentiable. Additionally, because of the large number of degrees of freedom, quintic splines allow to specify additional constrains on the trajectory: we choose to include in the trajectory segments where the acceleration is zero while maintaining 3-times differentiability of  $x$ ,  $y$ ,  $z$ . This gives a rest time to the pilot. Fig. 6 shows a trajectory generated in this manner. Note that the method allows to generate three dimensional flight paths. We present here two dimensional results for ease of representation. Six segments are used and the acceleration is set to zero between the second and third, and between the fourth and fifth control points. Although adequate to prescribe periods of zero acceleration, employing quintic spline is cumbersome because they are prone to oscillations in the vicinity of steep gradients. Besides, they require to specify second derivatives of  $x$ ,  $y$ ,  $z$  and  $V$  with respect to  $s$  at both start point  $s_1$  and  $s_N$ . This specification is not intuitive and greatly influences the flyability and comfort of the obtained trajectory. Accordingly, we have developed an alternative alleviating this problem.

This approach relies on cubic Bézier curves for the flight path. In order to obtain the higher order derivatives of the path needed for the subsequent flight mechanics computation, the Bézier curves are then interpolated with ordinary cubic splines. For the calculation of the acceleration, a spline on spline approach is used, i.e. the velocity vector is again approximated by cubic splines and this approximation is differentiated. Fig. 7 shows a trajectory generated in this

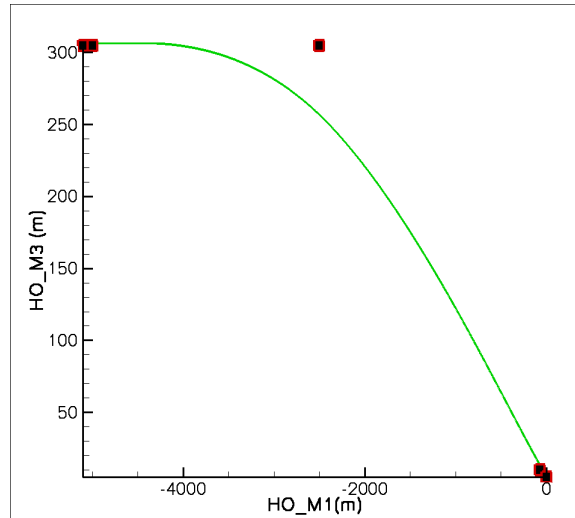


Fig. 7: Example of a trajectory generated from control points and cubic Bézier curves: altitude of helicopter versus horizontal distance to landing point. The control points are marked in red. The trajectory does not go necessarily through them.

manner. One obtains smooth curves but the trajectory does not pass through the control points. This, however, does not have negative consequences for the optimization procedure. A disadvantage of the Bézier spline approach is that zero acceleration intervals can only be achieved approximately using a proper choice of the control points. Nevertheless, because of their tremendous ease of use compared to the quintic splines, we use cubic Bézier curves in the rest of the paper.

We now assess the ability of the Bézier spline interpolation to reproduce a flown trajectory. The flight comprises a deceleration between time 34 s and 52 s, with a magnitude of 0.11 g. Fig 8 compares the measured flight with the flight reconstructed with Bézier curves and 95 control points picked on the measured path. Left is the altitude. Right shows the horizontal velocity. An excellent match can be observed. Note that here many control points have been used in order to reproduce an irregular flight path flown in reality. When using the trajectory generation module in the way it was conceived for (i.e. for trajectory design), much less control points are needed.

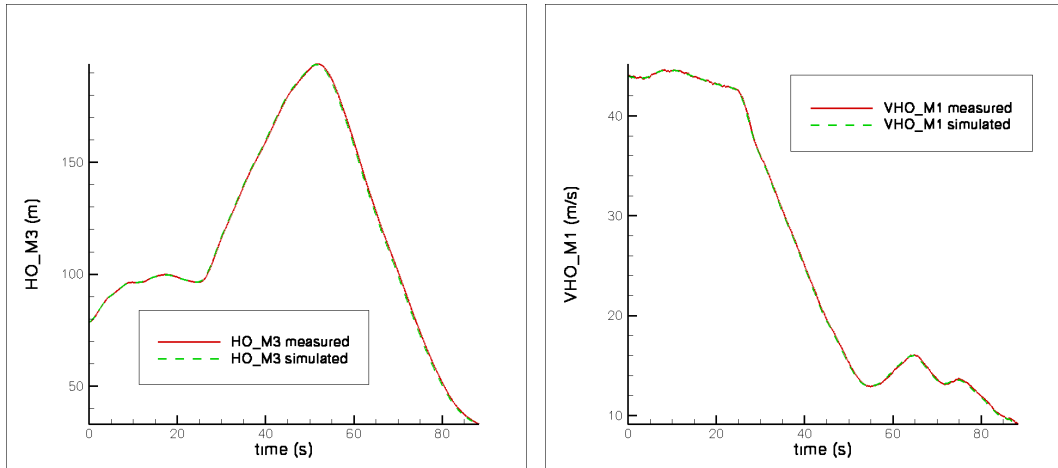


Fig. 8: Comparison of the measured flight and the flight reconstructed with Bézier curves and 95 control points picked on the measured path. Left, the vertical position HO\_M3 is plotted versus time. Right, the horizontal velocity VHO\_M1 is plotted versus time.

## FLYABILITY AND COMFORT

We first expose criteria and then explain how we check them.

### FLYABILITY

Guarantying the safety normally requires to avoid three states: 1) Vortex Ring State (VRS), 2) certain regions of the H-V (Height-Velocity) diagram in order to guaranty emergency landing in case of engine failure, 3) autorotation. For the EC135 at usual altitudes, there are no restriction due to H-V diagram. Thus, we restrict to checking avoidance of VRS and of autorotation:

\* VRS occurs when the helicopter flies in its own downwash. The velocity with respect to air is the determining parameter. As VRS is a purely aerodynamic phenomenon, the VRS avoidance criterion should be expressed in the helicopter coordinate system. This formulation is then also applicable for quasi-steady maneuvers. Therefore we express the standard VRS avoidance criterion in the H coordinate system, assuming that the standard criterion corresponds to flights in which H1 and H2 are approximately horizontal. For the EC135, VRS can occur if the projection on the plane of the helicopter floor (plane (H1H2)) of the helicopter velocity with respect to air is smaller than 9.5 m/s while this same velocity projected on the normal downward to this plane (i.e. along H3) is greater than 4 m/s.

\* Autorotation can lead to an increase of RPM and destruct the rotor. In HOST, the RPM is set constant and autorotation is modeled by a negative engine torque. In order to avoid autorotation, we require that the engine torque ratio (calculated

using the computed torque values of main and tail rotor) remains positive. Additionally, we ensure that the pilot can fly a trajectory by ensuring that the climb angle ( $\gamma$ ) is always larger than  $-15$  deg to avoid lack of visibility.

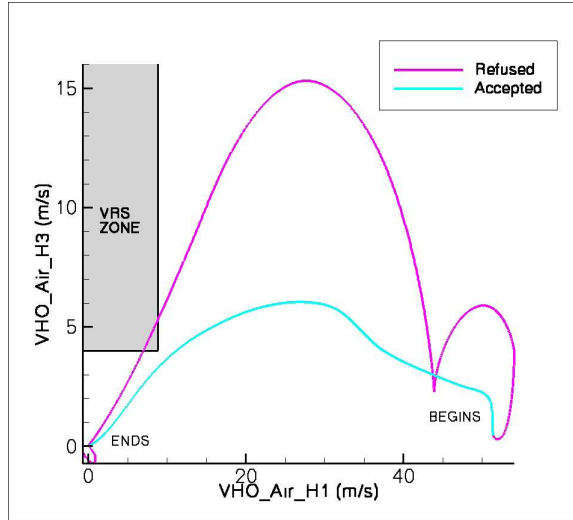


Fig. 9: Check of avoidance of the Vortex Ring State for two procedures. Time parametrizes both curves. The pink procedure enters the forbidden region and is thus rejected. It corresponds to the trajectory show in Fig. 6. The blue procedure corresponds to the procedure shown in Fig. 7. It satisfies avoidance of Vortex Ring State.

## COMFORT

High accelerations are rejected: the acceleration of the helicopter must remain between  $0.7$  g and  $1.3$  g.

Flyability and comfort checks necessitate variables still unknown after the trajectory generation which delivers only the Cartesian position of the helicopter and its time derivatives. We explain how we obtain those missing parameters.

We use once more the flight mechanics program in inverse simulation mode. Recall that an inverse simulation performs well if the objective variables are the rotational velocities (or accelerations) and the vertical velocity (or acceleration), or closely related variables. The vertical velocity is directly available from the time derivative of the flight path. We choose as additional objective variables  $\frac{d\phi}{dt}$ ,  $\frac{d\theta}{dt}$ , and  $\frac{d\psi}{dt}$ . Thus, for each point on the trajectory, we obtain first  $\psi, \theta, \phi$  by performing a trim with prescribed linear velocity and acceleration, and zero

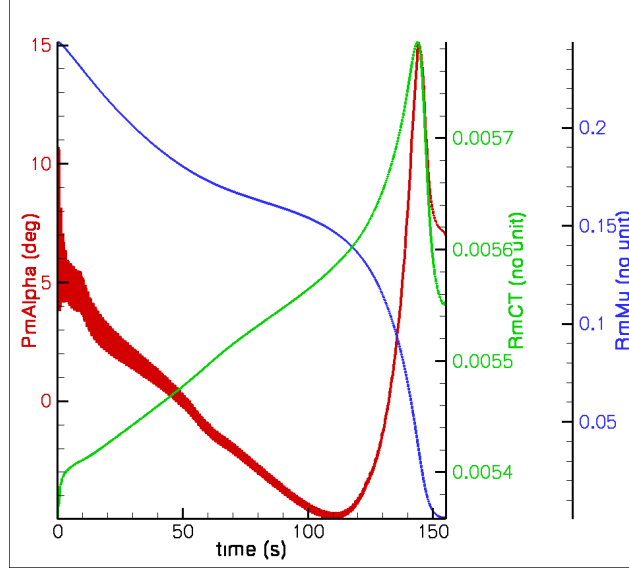


Fig. 10: Noise emission parameters for the trajectory shown in Fig. 11: tip path plane angle of attack of the main rotor  $\alpha_{P_m}$ ; advance ratio of the main rotor  $\mu_{R_m}$ ; thrust coefficient of the main rotor  $CT_{R_m}$ .

rotational velocity and acceleration. We set the heading so that the side-slip angle is approximately zero. For this trim, we also input values of mass, position of gravity center and wind. We output  $\theta, \phi$  and the four pilot commands. Repeating this procedure for all points on the trajectory, we obtain  $\frac{d\phi}{dt}$ ,  $\frac{d\theta}{dt}$ , and  $\frac{d\psi}{dt}$  and can perform an inverse simulation. The flight is now a real flight, and not simply a set of equilibriums with prescribed acceleration: the rotational velocities and accelerations can be non zero. We now know all variables needed to check the flyability. As example, Fig. 9 shows the forbidden VRS region and two procedures. The blue procedure (corresponding to Fig. 7) avoids VRS and is thus accepted while the pink one (Fig. 6) is rejected. A flyable and comfortable flight can now be fed to the subsequent steps of the ground noise computation.

## GENERATION OF NOISE EMISSION PARAMETERS

We recall that the whole noise evaluation relies on propagating the noise emitted at prescribed emission instants. The flight procedure is thus discretized. A time step of 1s is chosen as compromise between numerical cost and accuracy in the discretization of mild maneuvers. At each emission time, the flight mechanics program outputs the parameters ruling the noise emission. Fig. 10 shows as example the values of the noise emission parameters as function of time for the procedure generated with cubic Bézier curves and shown in Fig. 7.

We now illustrate the ability of Bézier cubic curves to reproduce the noise emission parameters of experimental data and of flight parameters measured on board. We consider again the flight shown in Fig. 8. The deceleration takes place time 34s and 52s. Fig. 11 (left) compares the pitch angle  $\theta$  measured on board with the value obtained after running the flight mechanics program in inverse mode on the cubic Bézier curves generated from 95 control points. Both values match very well. We now turn to the noise emission parameters. The experimental data is first completed with the flight mechanics program (procedure explained in the section "Generation of aeroacoustic database"). The values of the noise emission parameters obtained in this manner are referred to as "measured data". "Simulated data" refers to values obtained using Bézier curves. Fig. 11 (right) and 12 compare the measured and simulated values of the main rotor tip path plane angle of attack  $\alpha_{Pm}$ , main rotor thrust coefficient  $CT_{Rm}$  and main rotor advance ratio  $\mu_{Rm}$ . A very good agreement between measured and simulated data is observed for all noise emission variables. The procedure employed to obtain noise emission parameters starting from control points and cubic Bézier curve is thus valid.

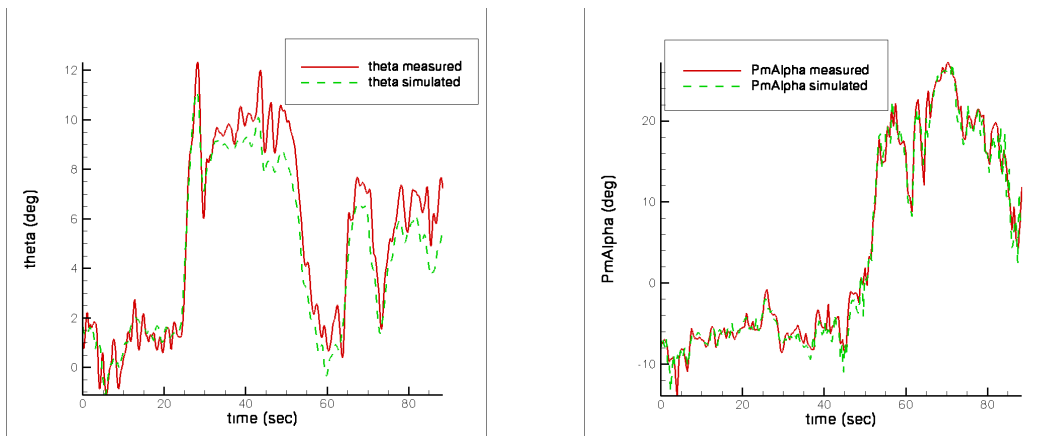


Fig. 11: Comparison between the measured and simulated pitch angle ( $\theta$ , left) and main rotor tip path plane angle of attack ( $\alpha_{Pm}$ , right) for the flight path shown in Fig. 8.

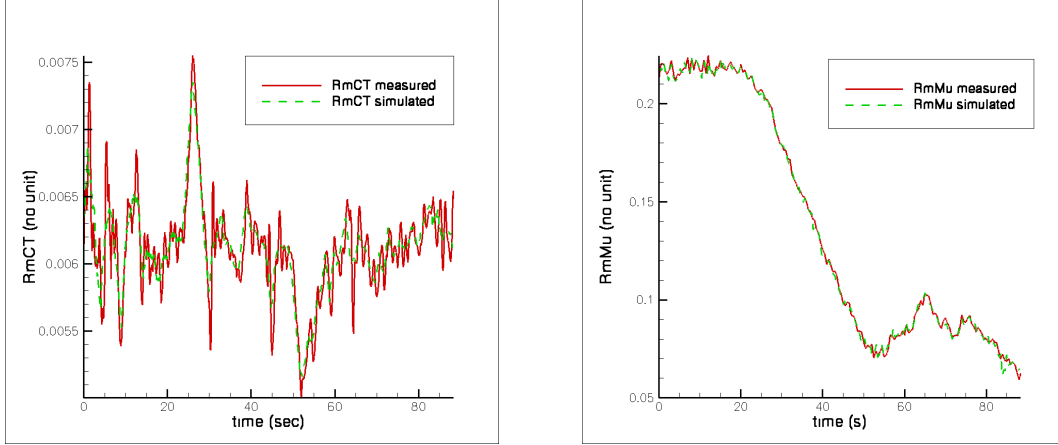


Fig. 12: Comparison between the measured and simulated main rotor thrust coefficient ( $CT_{Rm}$ , left) and main rotor advance ratio ( $\mu_{Rm}$ , right) for the flight path shown in Fig. 8.

## NOISE EMISSION

We consider a carpet of microphones set on the ground. Our goal here is to obtain the noise emission in the direction of each microphone for each emission time on the trajectory. Therefore, we rely on a double interpolation on directivity angles and on flight condition.

Recall that the three chosen noise emission parameters are the angle of attack of the main rotor tip path plane  $\alpha_{pm}$ , the advance ratio of the main rotor  $\mu_{Rm}$ , and the main rotor thrust coefficient  $CT_{Rm}$ . They form a noise emission triplet. We focus now on one emission instant and one ground microphone: the current value of the noise emission triplet is known. The vector joining emission point to microphone allows to obtain the directivity angles  $\theta_3$  and  $\phi_3$  (in the helicopter coordinate system). Our first goal is to retrieve from the aeroacoustic database the four measured noise emission with noise emission triplet closest to our current triplet. All noise emission parameters are adimensionalized so that their values vary between -1 and +1. We use a Delaunay triangulation to obtain an unstructured mesh, set of tetrahedra having the measured noise emission triplets as vertices. The tetrahedron including the current noise emission triplet is found and its barycentric coordinates within the tetrahedron computed. In the unlikely case that the current noise emission triplet is not within the scope of the database, its projection on the border of the database envelop is used. Then only three measured noise emission triplets are used to obtain the barycentric coordinates. We return to the usual case when four neighboring triplets are used.

For each of the four measured noise emission hemispheres, the noise emission must be obtained in the direction  $(\theta_3, \phi_3)$ . Note that the noise emission is known exactly only in the direction of the microphones used for the measurement (backpropagation explained in section “Acoustic Data”). We employ again a Delaunay triangulation. This requires using Cartesian coordinates: the directivity angles are transformed to  $\theta_3 \cos(\phi_3)$  and  $\theta_3 \sin(\phi_3)$ . Then a two dimensional triangulation is performed. The triangle including the current  $\theta_3 \cos(\phi_3)$ ,  $\theta_3 \sin(\phi_3)$  is found and its barycentric coordinates used as weighting of the measured noise emissions. Should the current  $\theta_3 \cos(\phi_3)$ ,  $\theta_3 \sin(\phi_3)$  be outside the envelope of measured directions, its projection on the envelope of the measured directivity angles is used.

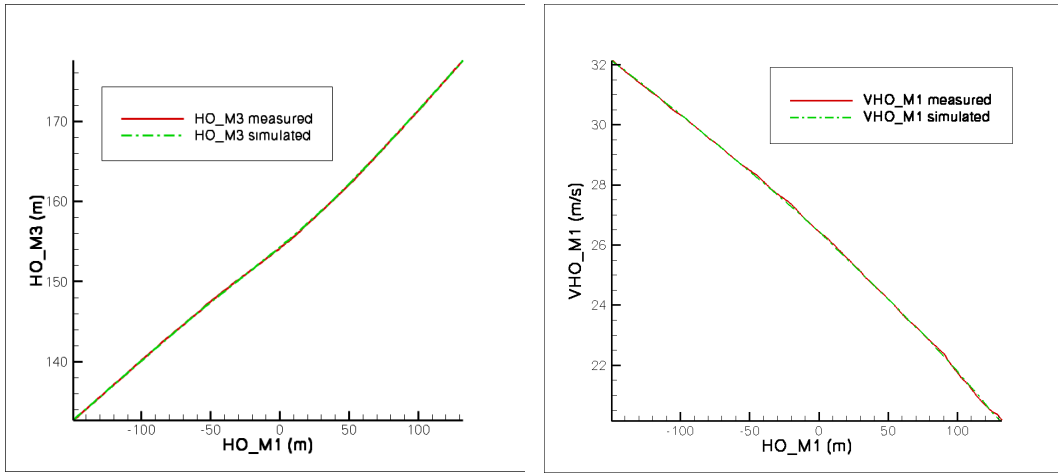


Fig. 13: Comparison of the measured flight and the flight reconstructed with the Bézier curve interpolation and 12 control points picked on the measured flight path. Left: the vertical position (HO\_M3) is plotted. Right: the horizontal velocity (VHO\_M1) is plotted. This figure isolates the deceleration of the flight shown in Fig. 8.

Repeating this for each vertex of the enclosing tetrahedron, four spectra (sound pressure level as function of frequency) are thus obtained. The final spectrum is obtained by interpolating the four spectra using the tetrahedron barycentric coordinates as weighting coefficient.

The procedure is repeated in the direction of all ground microphones. Then noise propagation is performed. The whole procedure is repeated by sweeping emission instants on the trajectory. Before turning to the final validation of ground noise footprint, we mention details of the noise propagation.

## NOISE PROPAGATION

For spherical spreading, atmospheric attenuation and Doppler effect, the same physical models as in the backpropagation explained in "Acoustic Data" are used.

## GROUND NOISE

This section is devoted to the final validation of the method: ground noise obtained by the computational chain is compared with measured ground noise. We consider the decelerated part (magnitude 0.11g) of the trajectory shown in Fig. 8. Fig. 13 shows a detailed view of the altitude and the horizontal velocity. Thus, the noise emission parameters vary as function of time. 12 control points are used for the simulated quantities. The experimental flight has been performed in the presence of a transverse wind varying around 8 m/s at helicopter height.

Fig 14 shows in red the measured sound pressure level (in dB) as function of time for two ground microphones located respectively at  $M1 = -224$  m,  $M2 = 0$  m and  $M1 = -129$  m,  $M2 = -74$  m. Additionally, two simulated noises are shown. One simulated noise (blue curve) uses the measured trajectory and the emission spheres constructed using this flight. This means that for each emission instant, the instantaneous ground noise is backpropagated unto a sphere and then repropagated down to the ground. 25 emission instants (and thus spheres) regularly distributed between first and last emission instants are used. This corresponds to a reception time step of about 0.3 s. The blue curve and the measured data (red) differ slightly because the emission instants are every 0.3 s and, for the simulation, the ground signal is interpolated in time between reception instants. Note that the ground model for forward and backward propagation is the same (calibrated plate model) in order to remove its effect. The second curve of simulated data (green curve) is more interesting: the complete ground noise footprint tool has been used: cubic Bézier curves have been used between the 12 control points. The emission time step is 1 s. The SPL curve matches the measured data within 2 dB. Note that the whole aeroacoustic database has been used: it contains flights that have been measured with different wind conditions. The effect of wind is taken into account only on noise emission parameters. Its effect on propagation is ignored: this results in a deficiency in the back / forward noise propagation in the presence of wind. We plan to use ray tracing in future work to alleviate this problem [5].

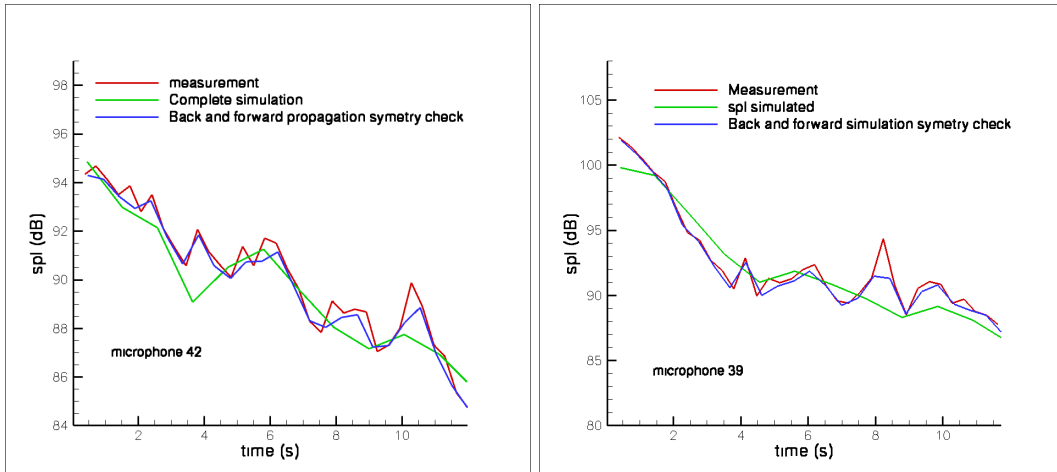


Fig. 14: Sound Pressure Level (SPL) in dB as function of reception time for the experimental data (red), the back- and forward-propagated noise (blue), and the fully simulated noise (green). Left: at a microphone set at  $M1=-224$  m,  $M2 = 0$  m. Right: at a microphone set at  $M1 = -129$  m,  $M2 = -74$  m.

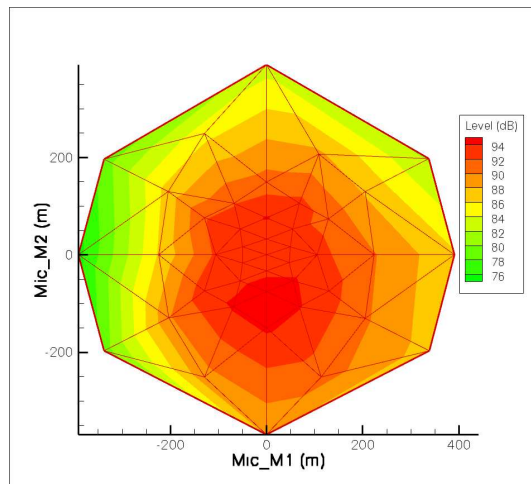


Fig. 15: Measured SEL level for the trajectory shown in Fig. 13.

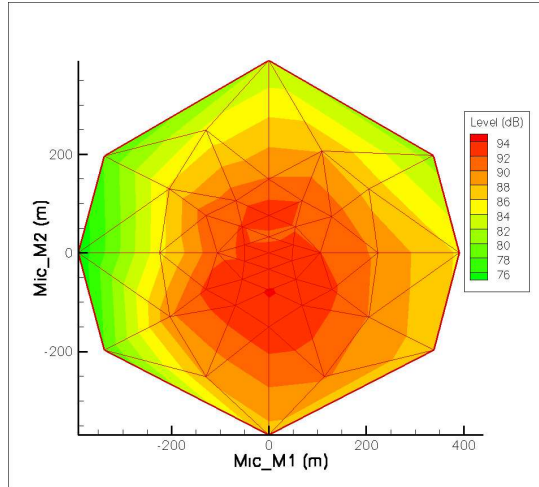


Fig. 16: Backward and forward propagated (same noise emission spheres) SEL level for the trajectory shown in Fig. 13.

In order to show results on larger ground surface, Fig. 15, 16 and 17 show the SEL levels for the same flight path segment for respectively the measured data, the partially simulated data (forward and backward propagation of the same noise emission spheres), and the data fully simulated with Bézier curves and the whole aeroacoustic database. All SEL levels are computed on different time range for each microphone. For a given emission time, the reception time indeed varies from one microphone to the other depending on the distance between emission point and microphone. For each microphone, the SEL is integrated between first and last own reception time. Again we note the good agreement of all three plots for the whole carpet of microphones. The whole computational chain is thus reliable to obtain the ground noise footprint of flights with acceleration / deceleration satisfying quasi steadiness. Differences between measured and fully simulated data are smaller than 2 dB. Such a difference is much smaller than the noise abatement expected from new flight procedure designs. Thus the computational method is appropriate for the design of noise abatement flight procedures including maneuvers.

Fig. 18 shows the application of the method for a flight not flown during the 2004 PAVE campaign. The flight path is shown in Fig. 7. The whole aeroacoustic database is used. The backpropagation distinguishes between grass and concrete microphones. The Ingard-Rudnik ground model is used for the forward propagation with same flow resistivity for all microphones. The whole computational chain has been run, including flyability and comfort (see Fig. 9). The microphone carpet counts 77 microphones and covers a rectangular surface of 6000 m times 4000 m. The total computational time is approximately 20 minutes on a home PC (the computational time to generate the complete aeroacoustic database is approximately 18 CPU hours). Because of its rapidity, the computational chain can be run a very large number of times within a reasonable amount of time. Concerning the computational cost, the tool is thus appropriate for the design of low-noise flight procedures. It was recently associated with an optimizer in the Friendcopter EU project to design low noise flight procedures which have been acoustically tested in flight [14].

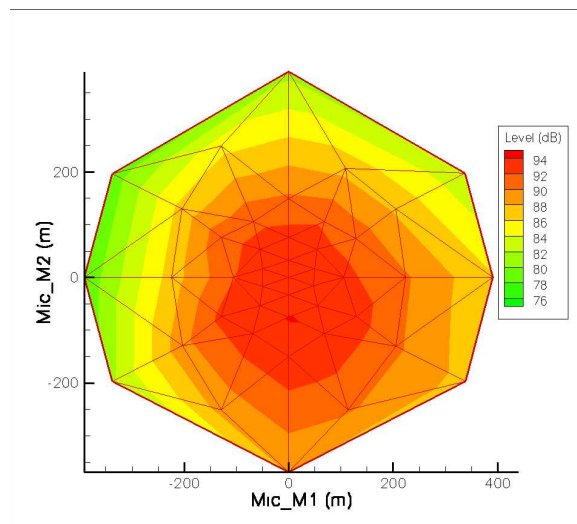


Fig. 17: Fully simulated SEL level for the trajectory shown in Fig. 13.

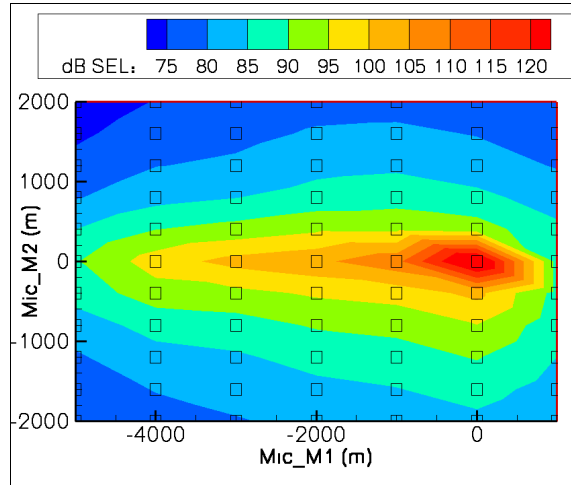


Fig. 18: Ground noise footprint (SEL level) for the complete flight shown in Fig. 7.

## CONCLUSIONS

In this paper we have presented a tool able to compute the ground noise footprint generated by a whole helicopter in an arbitrary flight. We use a hybrid approach: generation of an arbitrary trajectory, checks of flyability and comfort, and propagation of noise down to the ground are performed numerically whereas noise emission characteristics are provided by an experimental aeroacoustic database, resulting of postprocessing of the flight campaign PAVE 2004.

The paper contains a description of the generation of the aeroacoustic database with a flight mechanics program and a backpropagation tool. The extent of the database (range of noise emission parameters) is shown. We explain the method used to compute the ground noise footprint of arbitrary, comfortable and flyable flights. In particular we discuss how measured data is selected and interpolated from the aeroacoustic database. Parameterizing the noise emission by the instantaneous value of three aerodynamic parameters (main rotor tip path plane  $\alpha_{pm}$ , advance ratio of the main rotor  $\mu_{Rm}$ , and main rotor thrust coefficient  $CT_{Rm}$ ) appeared adequate to simulate ground noise footprint for quasi-steady maneuver flights. For a deceleration of 0.11 g, good agreement between measured and simulated data was shown. The tool is thus appropriate to study the influence of moderate deceleration / accelerations on noise emission and use their potential for design of noise abatement flight procedures. How the tool was used together with an optimizer to design quiet flights, tested in flight in summer 2008 (first results in [14]), will be explained in future publications.

## ACKNOWLEDGEMENTS

The authors wish to thank M. Adler (DLR), B. Benoit (Eurocopter), B. Claret (Eurocopter) and W. von Grünhagen (DLR) for their always competent and friendly help with HOST. They thank J. Yin (DLR) for the performance of UPM computations. They also greatly appreciated the support of L. Meliveo (Anotec Consulting).

This work has been supported by the European Union and the German Ministry of Education and Research (project Friendcopter) and the German Ministry of Defense (project PAVE and PAVE2).

## BIBLIOGRAPHY

- [1] Bass, H. E.; Sutherland, L. C. and Zuckerwar, A. J., "**Atmospheric Absorption of Sound Update**" Journal of the Acoustical Society of America, Vol. 88, No. 4, 1990, pp. 2019-2021.
- [2] Benoit, B.; Dequin, A.-M.; Kampa, K.; Gruenhagen, W.; Basset, P.-M. and Gimonet, B., "**HOST: A General Helicopter Simulation Tool for Germany and France**", 56th American Helicopter Society Annual Forum, Virginia Beach, Virginia, USA, May 2000.
- [3] Delany, M. E. and Bazley, E. N., "**Acoustical properties of fibrous absorbant materials**" Applied Acoustics, Vol. 3, 1970, pp. 105-106.
- [4] Le Duc, A.; Spiegel, P.; Guntzer, F.; Lummer, M.; Buchholz, H. and Götz, J., "**Simulation of complete helicopter noise in maneuver flight using aeroacoustic flight test database**", 64th American Helicopter Society Annual Forum, Montréal, April-May 2008.
- [5] Lummer, M., "**Maggi-Rubiniwicz Diffraction Correction for Ray-Tracing Calculations of Engine Noise Shielding**", AIAA-paper 2008-3050, Vancouver, 2008.
- [6] Perez, G. and Costes, M., "**A New Aerodynamic & Acoustic Computation Chain for BVI Noise Prediction in Unsteady Flight Conditions**", American Helicopter Society 60th Annual Forum, Baltimore, MD, USA, June 2004.

- [7] Pott-Pollenske, M.; Dobrzynski, W.; Buchholz, H.; Guérin, S.; Saueressig, G. and Finke, U., "**Airframe Noise Characteristics from Flyover Measurements and Predictions**", AIAA/CEAS Paper 2006-2567, 2006.
- [8] Prieur, J.; Costes, M. and Bader, J. D., "**Aerodynamic and acoustic calculations of transonic nonlifting hovering rotors**", AHS Technical Specialists Meeting on Rotorcraft Acoustics and Fluid Dynamics, Philadelphia, PA, U.S.A., October 1991.
- [9] Rudnick, I., "**The propagation of an acoustic wave along a boundary**" Journal of the Acoustical Society of America, Vol. 19, No. 2, 1947, pp. 348-356.
- [10] Schmitz, F. H.; Gopalan, G. and Sim, B. W.-C., "**Flight Trajectory Management to Reduce Helicopter Blade-Vortex Interaction (BVI) Noise with Head/Tailwind Effects**", 26th European Rotorcraft Forum, The Hague, The Netherlands, September 2000.
- [11] Schultz, K.-J. and Splettstoesser, W. R., "**Measured and predicted impulsive noise directivity characteristics**", 13th European Rotorcraft Forum, Arles, France, 1987.
- [12] Spiegel, P.; Buchholz, H. and Pott-Pollenske, M., "**Highly Instrumented BO105 and EC135-FHS Aeroacoustic Flight Tests including Maneuver Flights**", American Helicopter Society 61st Annual Forum, Grapevine, TX, June 1-3, 2005.
- [13] Spiegel, P.; Buchholz, H. and Splettstoesser, W., "**The "RONAP" Aeroacoustic Flight Tests with a Highly Instrumented BO 105 Helicopter**", American Helicopter Society 59th Annual Forum, Phoenix, Arizona, May 2003.
- [14] Spiegel, P.; Guntzer, F.; Le Duc, A.; Buchholz, H., "**Aeroacoustic flight test analysis and guidelines for noise-abatement-procedure design and piloting**", 34th European Rotorcraft Forum, Liverpool, United Kingdom, September 2008.
- [15] Splettstoesser, W. R.; Kube, R.; Wagner, W.; Seelhorst, U.; Boutier, A.; Micheli, F.; Mercker, E. and Pengel, K., "**Key Results from a Higher Harmonic Control Aeroacoustic Rotor Test (HART)**" Journal of the American Helicopter Society, Vol. 42, No. 1, January, 1997.

- [16] Yin, J. and Ahmed, S. R., "**Aerodynamics and Aeroacoustics of Helicopter Main-Rotor/Tail-Rotor Interaction**", AIAA paper No. AIAA-99-1929, 1999, 1999.
- [17] Yin, J. and Buchholz, H., "**Toward Noise Abatement Flight Procedure Design: DLR Rotorcraft Noise Ground Footprint Model**" Journal of the American Helicopter Society, Vol. 52, No. 2, April 2007, pp. 90-98.
- [18] Yin, J.; Spiegel, P. and Buchholz, H., "**Towards Noise Abatement Flight Procedure Design: DLR Rotorcraft Noise Ground Footprint Model and its Validation**", 30th European Rotorcraft Forum, Marseille, France, September 2004.